



8<sup>th</sup> International Conference on Photonic Technologies LANE 2014

## Electro-optic KTN devices

Shogo Yagi<sup>a,\*</sup>, Kazuo Fujiura<sup>a</sup>

<sup>a</sup>NTT Advanced Technology Corporation, 3-1 Morinosato Wakamiya, Atsugi, Kanagawa 243-0124 Japan

- Invited Paper -

---

### Abstract

We have grown KTN crystals with optical quality, and developed high-speed beam deflectors and variable focal length lenses based on KTN's large electro-optic effect. Furthermore, by using the KTN beam deflectors, we have developed a swept light source for OCT operable at 200 kHz.

© 2014 Published by Elsevier B.V. This is an open access article under the CC BY-NC-ND license

(<http://creativecommons.org/licenses/by-nc-nd/3.0/>).

Peer-review under responsibility of the Bayerisches Laserzentrum GmbH

**Keywords:** Kerr effect; beam deflector; variable focal length lens; swept light source

---

### 1. Introduction

The KTN is an abbreviation of the chemical formula of potassium tantalate niobate,  $K(\text{Ta}_{1-x}\text{Nb}_x)\text{O}_3$ . In spite of its large electro-optic effect, it took more than 50 years after its discovery by Trieswasser (1959) for the crystal to be commercially available (Fig.1). This stems from the difficulty in crystal growth, which was overcome by precise temperature control with a sufficient suppression of temperature gradient.

Unlike other electro-optic oxides such as  $\text{LiNbO}_3$  and  $\text{BaTiO}_3$ , the KTN is usually operated in its cubic phase after Geusic (1964), whose inversion symmetry nullifies the first order electro-optic effect or Pockels effect and hence the second order, Kerr effect, becomes dominant. Although the electro-optic effect generally gets weak when its order is higher, the divergence of the dielectric constant near the phase transition temperature compensates it in

---

\* Corresponding author. Tel.: +81-46-250-3771; fax: +81-46-250-3871.

E-mail address: [shogo.yagi@ntt-at.co.jp](mailto:shogo.yagi@ntt-at.co.jp)

the case of KTN. We usually operate the KTN devices at a temperature where the relative dielectric constant is 17,500. Because of the steep dependence on temperature, the KTN devices require temperature control.

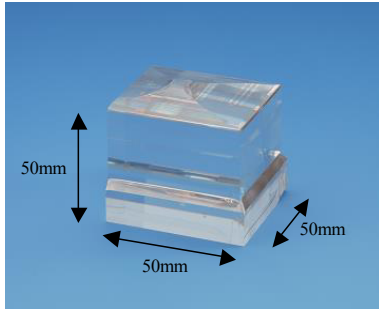


Fig. 1. KTN crystal grown at NTT-AT.

Also, the large dielectric constant makes it easy for electrons to penetrate into KTN when the external voltage is applied as Nakamura (2006) indicated. It makes us to consider two types of electro-optic effects for developing KTN devices.

When the electrodes are made of platinum, the Schottky barrier between the electrode and the KTN blocks electron injection. In this case, the electro-optic effect can be calculated according to the conventional Kerr effect (Chen (1966)). The KTN variable focal length lenses are based on this effect as Imai (2011, 2012) described.

On the other hand, when titanium electrode is employed, the Schottky barrier is not enough high to prevent the electron injection. In this case, the sum of the electric field generated by the injected electrons and the external field becomes the effective field for changing the refractive index. The KTN deflectors are based on this effect as Miyazu (2011) described.

## 2. Electro-optic effect of the KTN

When the electric field of light is parallel to the electrostatic electric field ( $EE$ ) in KTN, the index modulation ( $\delta n$ ) due to the electric field via the Kerr effect is given by

$$\delta n = -\frac{1}{2} n^3 \varepsilon^2 g_{11} E^2 \quad (1)$$

where  $n$  and  $g_{11}$  are the refractive index and the electro-optic constant of KTN respectively, which are independent of temperature while they have wavelength dispersion. Their product,  $n^3 g_{11}$  exceeds  $2 \text{ m}^4/\text{C}^2$  at wavelengths shorter than 500 nm with steep wavelength dependence while it stays around  $1 \text{ m}^4/\text{C}^2$  in the infrared region.

The dielectric constant,  $\varepsilon$ , depends on temperature ( $T$ ) following Curie-Weiss law

$$\varepsilon = \frac{140000 \varepsilon_0}{T - T_c} \quad (2)$$

where  $\varepsilon_0$  is the dielectric constant in vacuum and  $T_c$  is the Curie temperature that is a few Celsius below the real phase transition temperature. For most applications, we set the KTN temperature so that its relative dielectric constant is 17500, which gives us  $T = T_c + 8$  and  $\partial \varepsilon / \partial T = -2190 \varepsilon_0$ , where  $\delta n$  can be controlled within 2.5 % precision by controlling the temperature with 0.01 C precision.

When the electrode is made of a metal whose work function is small such as Ti, electrons are injected into the KTN crystal, and hence the electrostatic field generated by the internal electrons must be taken into account in eq. (1). Assuming the true charge density,  $\rho_0$ , is uniform throughout the KTN crystal [see Imai, et.al (2014)], the index modulation under the applied voltage  $V$  is given by

$$\delta n = -\frac{n^3}{2} g_{11} \left( \rho_0 x + \frac{\varepsilon V}{d} \right)^2 \quad (3)$$

where  $x$  axis is taken normal to the electrodes, and its origin is located at the midpoint of the electrodes with a gap of  $d$ . Since eq.(3) tells the index has a parabolic modulation in terms of position, the charged KTN acts as a cylindrical convex lens whose optical axis displaces proportional to the applied voltage.

### 3. KTN beam deflector

In order to inject electrons into the KTN crystal uniformly, we apply plus and minus DC voltages for a few seconds before beam deflection operation. The injected electrons remain trapped in the KTN until they are intentionally photo-excited by a UV light exposure for a few seconds. This photo-excitation sets the shortest limit of wavelength at 488 nm when input power is 5 mW. When the wavelength gets longer, the maximum input power can be larger because the photo-excitation can hardly occur. For example, the deflection angle does not show any degradation by exposing 1.06  $\mu\text{m}$  1.06  $\mu\text{m}$  wavelength CW light with the power of 9 W at 0.5 mm in diameter. For high peak pulses, the damage threshold was around 10 J/cm<sup>2</sup> when 10 ns pulse was exposed.

Then, the lens power of the charged KTN must be compensated with cylindrical concave lenses when the deflected beam needs to be collimated. Figure 2 shows the far field beam profiles during continuous beam scanning at 100 kHz, where the pulsed collimated incident beam diameter is 0.5 mm (1/e<sup>2</sup>). Figure 3 shows the voltage dependence of the deflection angle, where each point corresponds to the center of the spot in Fig.2.

As long as the time response is concerned, the electron mobility and the current limit of voltage supply must be considered for low and high frequencies, respectively.

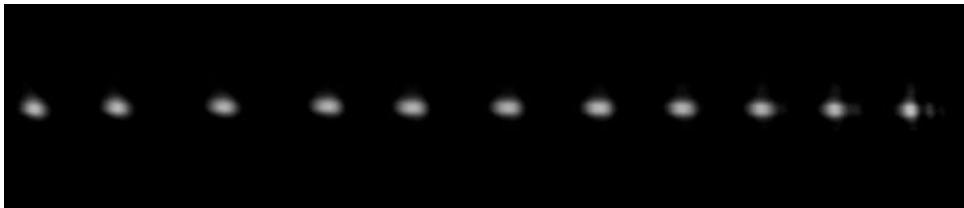


Fig. 2. Far field beam profiles deflected at 100 kHz. Each spot corresponds to the point in Fig. 3.

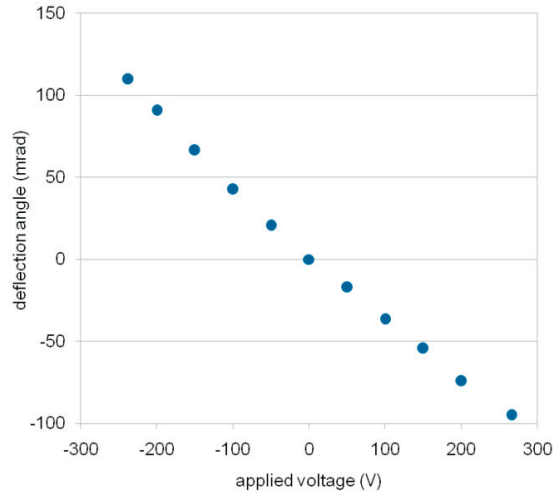


Fig. 3. Voltage dependence of deflection angle.

Since the electron mobility is around  $1.28 \times 10^{-4} \text{ cm}^2/\text{Vs}$  according to Katsura (2012), electrons can travel 1 mm in 0.26 sec under the typical external field of 300 V/mm. 300 V/mm This means the assumption of uniform charge density in eq.(3) is no longer valid for the low frequency, and the beam profiles are deteriorated by complicated time-dependent charge distribution. Therefore, we use the KTN deflector at frequencies higher than 100 Hz.

For higher frequencies, the flat frequency response of the beam deflection up to 400 kHz has been confirmed by Miyazu (2010). Major obstacle to achieve much higher frequency is in a voltage supply. Because of the large dielectric constant, a KTN chip has the electro-static capacitance of around 2 nF, which requires the current of 1.9 A when  $\pm 300 \text{ V} \pm 300 \text{ V}$  is applied at 500 kHz. In spite of the large current necessity, the energy consumption is minimized by using resonant circuit. We have designed and developed resonant type power supplies for 100 kHz and 200 kHz. Although the frequency is fixed, its waveform can be arbitrarily designed by superposing its harmonics set to appropriate amplitudes and phases.

The number of resolvable spots,  $N_R$ , is given by

$$N_R = \frac{\Theta D}{2\lambda} \quad (4)$$

where  $\Theta$ ,  $D$  and  $\lambda$  are the full deflection angle, the deflected beam diameter and wavelength, respectively. Since the thickness of KTN sets a limit to the beam diameter, it should be as large as possible for increasing a resolution. However, it makes difficult to inject electrons uniformly throughout the crystal because the electric field generated by the injected electrons hinders additional injection. Therefore, we have widened the full deflection angle by adopting a 3-pass geometry while we set the thickness limit at 1.2 mm. Figure 4 shows the 3-pass geometry, in which the light bounces twice inside the crystal to triple the full deflection angle compared with one-pass geometry.

Figure 5 shows the KTN chip (3 x 4 x 1 mm) used for 3-pass geometry.

Figure 6 shows the 1-D KTN deflector module in which the temperature controlling system is installed. The incident light is guided by a PM fiber and collimated in front of the KTN chip. Also, the lens power of the KTN is compensated by a cylindrical concave lens so that the deflected beam is collimated.

By using two KTN chips and a half-wave plate between them, a 2-D KTN deflector can be assembled as well.

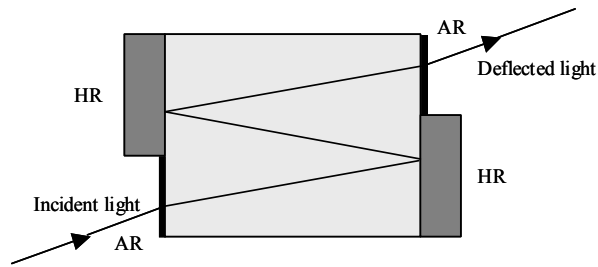


Fig. 4. Optical path of 3-pass KTN deflector.

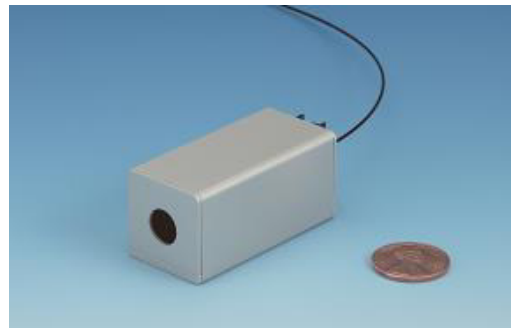


Fig. 5. KTN chip used for 3-pass KTN deflector; Fig. 6 KTN deflector module.

#### 4. KTN variable focal length lens

Unlike the deflectors, the electron injection does not take place in the KTN varifocal lens. Fig.7 shows the structure of the KTN varifocal lens that consists of a KTN rectangular cuboid (6.6 x 6.6 x 4 mm) and 4 parallel platinum electrodes. The large work function of platinum builds the Schottky barrier at the interface between platinum and KTN to block the electron injection.

The light beam enters in the KTN face (6.6 x 4 mm) having no electrodes between #1 and #3 electrodes while it exits from the face between #2 and #4 electrodes.

The KTN varifocal lens acts as a cylindrical convex lens when the electric field of light is in the paper plane, because  $g_{11}$  is employed. To make a circular varifocal lens, two KTN chips are used in tandem.

Figure 8 show a varifocal lens module in which two KTN chips are installed in tandem to make a circular lens. Figure 9 shows the focused beam profiles with an assist lens of  $f = 250$  mm when various DC voltages are applied. Unlike the KTN deflector, the KTN varifocal lens can work from 0 Hz because no electron injection takes place.

For high frequency, we have confirmed a rapid response down to 1  $\mu$ s. Since its electrostatic capacitance is 1 nF, the power supply must provide a large current like the case for the KTN deflector. Multiple modules of varifocal lens can be stacked to enhance the lens power.

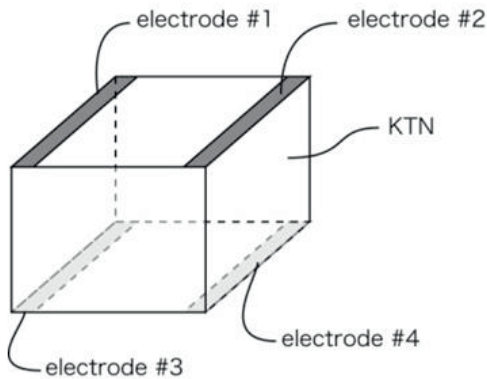
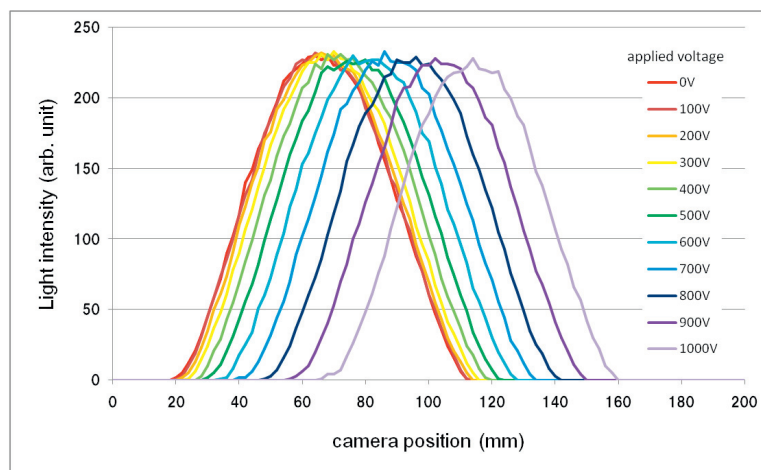


Fig. 7. Illustration of KTN varifocal lens chip.



Fig. 8. Picture of a KTN varifocal lens module.

Fig. 9. Focused beam profiles with an assist lens of  $f = 250$  mm under DC voltages application between 0 and 1000 V.

## 5. 200 kHz Swept light source

The swept light source is an application of the KTN deflector, which exploits the advantage of KTN's fast response. The swept light source is used for high speed optical coherence tomography (OCT), which can capture 3-D images from inside of optical scattering material such as human tissue. We adopt the Littman-Metcalf type external cavity LD (Fig. 10) in which the KTN deflector is used as the wavelength sweep engine [Okabe (2013) and Yagi (2012)].

To apply voltages to KTN, a resonant power supply of 200 kHz is employed. The center wavelength is 1310 nm and the sweep span is 100 nm.

The point spread function (PSF) is given in Fig.11. Satisfactory coherence length of our light source is demonstrated with a sample having a large depth such as shown in Fig. 12, where horizontal field of the view is approximately 3 mm.

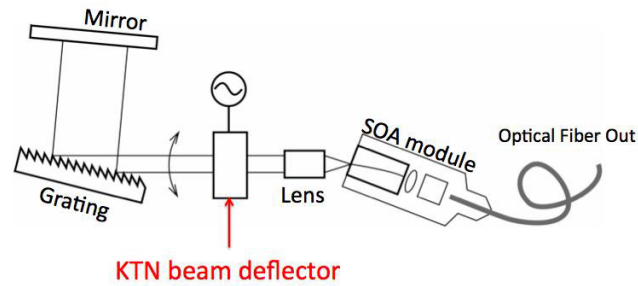


Fig. 10. Littman-Metcalf type external cavity LD equipped with the KTN deflector.

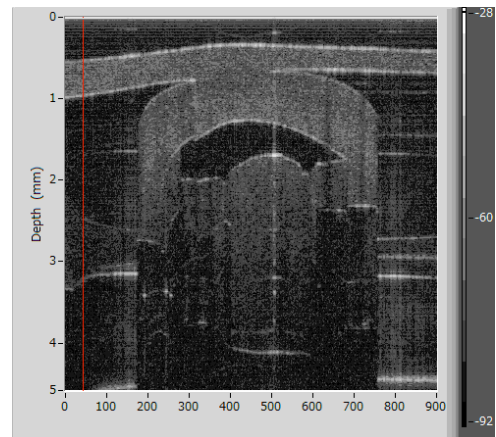
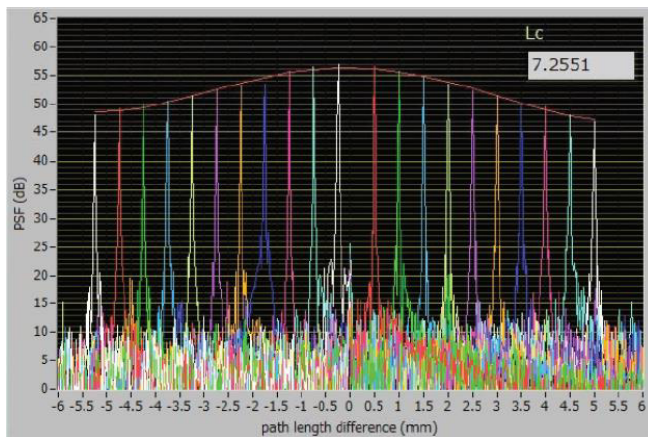


Fig. 11. Point spread function of the 200 kHz swept light source; Fig. 12 OCT image of zipper seal part of a vinyl bag.

## 6. Conclusion

We have grown the KTN crystals with optical quality, with which we have developed the beam deflectors operable between 100 Hz and 400 kHz, the varifocal lens responding down to 1  $\mu$ s. By using the KTN beam deflector, we have developed the swept light source for OCT operable at 200 kHz.

## References

- S. Trieswasser, "Study of ferroelectric transition of solid-solution single crystals of  $\text{KNbO}_3\text{-KTaO}_3$ ," *Phys. Rev.* 114(1), 63-70(1959)
- J. E. Geusic, S. K. Kurtz, L. G. Van Uitert, and S. H. Wemple, "Electro-optic properties of some  $\text{ABO}_3$  perovskites in the paraelectric phase," *Appl. Phys. Lett.* 4(8), 141-143(1964)
- K. Nakamura, J. Miyazu, M. Sasaura, and K. Fujiura, "Wide-angle, low-voltage electro-optic beam deflection based on space-charge-controlled mode of electrical conduction in  $\text{KTa1-xNb}_x\text{O}_3$ ," *Appl. Phys. Lett.* 89(13), 131115(2006)
- F. S. Chen, J. E. Geusic, S. K. Kurtz, J. G. Skinner, and S. H. Wemple, "Light modulation and beam deflection with potassium tantalite-niobate crystals," *J. Appl. Phys.* 37(1), 388-398(1966)
- T. Imai, S. Yagi, S. Toyoda, J. Miyazu, K. Naganuma, M. Sasaura, and K. Fujiura, "Fast Response Variable Focal-Length Lenses Using  $\text{KTa1-xNb}_x\text{O}_3$  Crystals," *Applied Physics Express* 4(2011)022501
- T. Imai, S. Yagi, S. Toyoda, J. Miyazu, K. Naganuma, S. Kawamura, M. Sasaura and K. Fujiura, "Fast response varifocal lens using  $\text{KTa1-xNb}_x\text{O}_3$  crystals and a simulation method with electrostrictive calculations," *Applied Optics* Vol. 51, Iss. 10, pp. 1532-1539 (2012)
- J. Miyazu, T. Imai, S. Toyoda, M. Sasaura, S. Yagi, K. Kato, Y. Sasaki, and K. Fujiura, "New beam scanning model for high-speed operation using  $\text{KTa1-xNb}_x\text{O}_3$  crystals," *Appl. Phys. Express* 4(11), 111501(2011)
- T. Imai, Jun Miyazu and J. Kobayashi, "Measurement of charge density distributions in  $\text{KTa1-xNb}_x\text{O}_3$  optical beam deflectors," *Optical Materials express* Vol.4 No.5 pp.976- 981(2014)

- Y.Katsura, T. Imai, J. Miyazu, S. Yagi, and H.Tsuda, "Mobility Evaluation in KTN Crystals by Retardation Measurements," *proc.IEICE* 2012, C-4-21 (in Japanese)
- J. Miyazu, Y. Sasaki, K.Naganuma, T. Imai, Seiji Toyoda, T.Yanagawa, M.Sasaura, S. Yagi, and K.Fujiura, "400 kHz Beam Scanning Using KTa<sub>1-x</sub>Nb<sub>x</sub>O<sub>3</sub> Crystals," *Proc. CLEO CTuG5* (2010)
- Y. Okabe, Y. Sasaki, M. Ueno, T. Sakamoto, S. Toyoda, J. Kobayashi, and M. Ohmi, "High-speed optical coherence tomography system using a 200-kHz swept light source with a KTN deflector," *Opt. Photon J.* 03(02), 190-193(2013)
- S. Yagi, K. Naganuma, T. Imai, Y. Shibata, J. Miyazu, M. Ueno, Y. Okabe, Y. Sasaki, K. Fujiura, M. Sasaura, K. Kato, M. Ohmi, and M. Haruna, "Improvement of coherence length in a 200-kHz swept light source equipped with a KTN deflector," *Proc. SPIE* 8213, 821333(2012)